

# Comparison of Theoretical Basics of Microphone and Piezoelectric Photothermal Spectroscopy of Semiconductors

J. Zakrzewski<sup>1</sup>  · M. Maliński<sup>2</sup> · Ł. Chrobak<sup>2</sup> ·  
M. Pawlak<sup>1</sup>

Received: 19 November 2015 / Accepted: 8 October 2016 / Published online: 7 November 2016  
© The Author(s) 2016. This article is published with open access at Springerlink.com

**Abstract** Photothermal spectroscopy has found a wide range of applications as a method of monitoring thermal, optical and recombination parameters of semiconductors. We consider microphone detection, widely used in photoacoustic spectroscopy, and piezoelectric detection. Both methods require knowledge of the temperature distribution in the sample and in its surroundings, the support surface and gas. For the microphone signal, we simulated the temperature at one of the sample surfaces; for the piezoelectric signal, we simulated the spatial temperature distribution orthogonal to the sample surface. We modeled an idealized semiconducting sample and one with surface defects. We found that the amplitude and phase spectra vary between the methods, enabling determination of optical and thermal parameters.

**Keywords** Microphone detection · Piezoelectric detection · Photothermal Spectroscopy · Semiconductors

## 1 Introduction

Photothermal spectroscopy has been developed to investigate the thermal and optical properties of semiconductors [1–3] since it is very sensitive and is complementary to

---

This article is part of the selected papers presented at the 18th International Conference on Photoacoustic and Photothermal Phenomena.

---

✉ J. Zakrzewski  
jzakrzew@fizyka.umk.pl

<sup>1</sup> Institute of Physics, Nicolaus Copernicus University, ul. Grudziądzka 5/7, 87-100 Toruń, Poland

<sup>2</sup> Department of Electronics and Computer Science, Technical University of Koszalin, ul. Śniadeckich 2, 75-453 Koszalin, Poland

absorption and photoluminescence spectroscopy. The most frequently used detection method in photothermal spectroscopy is the microphone method, in which periodic changes of surface temperature are measured by a microphone that detects changes of the gas pressure in the photoacoustic chamber [4]. The theory of photothermal response was proposed by Rosencwaig and Gersho [4] and was extended to a two-layer case by Fernelius [5]. In piezoelectric detection, the stress and strain of a sample due to the absorption of electromagnetic radiation are detected by a piezoelectric transducer. The first model of piezoelectric theory was advanced by Jackson and Amer [6], but their mathematical techniques were complicated, which discouraged their use in practical spectroscopy. Blonskij et al. [7] introduced a simpler approach that they proposed to apply to the determination of thermal diffusivity of solids. The temperature spatial distribution based on the idea of Bennett and Patty [8] was used by Malinski [9]. For both methods of detections, microphone and piezoelectric, it is necessary to consider the temperature distribution in the sample–support–gas system [4]. For microphone detection, one must know the temperature on the surface of the sample and for piezoelectric detection, the spatial distribution orthogonal to the sample surface must be known.

Both of these methods, microphone and piezoelectric, have the same basis—the temperature distribution, but the method of detection introduces differences in the solution describing the response of the detector.

Theories of the photoacoustic effect in semiconductors have been the subject of interest of much research [10–15] but have not been applied to spectroscopy - measurements of radiation intensity as a function of wavelength; they have usually been used to investigate transport parameters in the frequency domain experiments.

There are three sources of the thermal waves and as a result of the photoacoustic signal in semiconductors: fast thermalization of carriers in the conduction band, nonradiative bulk recombination of carriers that diffuse in the crystal and the nonradiative surface recombination of carriers [11, 13, 15]. In photoacoustic investigation of transport in semiconductors, one can also take into account immediate thermalization of carriers and nonradiative surface recombination [15]. In this article we decided to apply only the basic phenomenon: periodic heat flow in the solid sample being the result of a fast thermalization of carriers. The influence of the other terms will be taken into account in the future work. The main interest of our investigations is semiconductors of the A<sub>2</sub>B<sub>6</sub> group. In this case, the lifetimes of generated carriers are short in comparison to silicon and for low frequencies of modulation, the carriers phenomena do not play a role as important as in the case of silicon or germanium [16, 17].

Piezoelectric spectroscopy has already been used for the investigations of II–VI semiconductors [18]. These semiconductors are very promising materials from the point of view of application in construction of visible radiation sources in green laser diodes, spintronics, photodetectors and other applications in modern optoelectronics [19, 20]. It is very important from the application point of view that ternary and quaternary II–VI compounds allow an almost smooth change of the bandgap and lattice constant values [21] (bandgap and lattice constant engineering).

The goal of this article is to compare the theoretical basics of piezoelectric and microphone spectroscopy to assist in the interpretation of experimental data. Simulations of both methods are presented, for ideal and nonideal semiconductors.

The temperature distributions applied in the article were presented before in the case of piezoelectric detection [22]. In this article we use the theory in more detail, show the simulations for different (front and rear) configurations of piezoelectric detection and compare them to the microphone one. The simulations calculated for fixed parameters of bulk and surfaces of the sample show the similarities and differences of the phase and amplitude spectra for two methods and three configurations. Such a comparison was not done before yet and it should be helpful for the comparison and interpretations of experimental data.

### 1.1 Rosenzwaig–Gersho (RG) Theory

In R–G theory [4], the temperature field in the sample is given as a time-independent part of the solution for heat diffusion equation:

$$T_s(x) = U \exp(\sigma_s x) + V \exp(-\sigma_s l) - E \exp(\beta x) \tag{1}$$

$$E = \frac{A}{(\beta^2 - \sigma_s^2)} = \frac{\beta I_0}{2k_s(\beta^2 - \sigma_s^2)}. \tag{1a}$$

$$U = E \frac{(r + g)(1 + b) \exp(\sigma_s l) - (r - b)(1 - g) \exp(-\beta l)}{D}, \tag{1b}$$

$$V = E \frac{(r + g)(1 - b) \exp(-\sigma_s l) - (r - b)(1 + g) \exp(-\beta l)}{D}, \tag{1c}$$

$$D = \exp(\sigma_s l)(1 + g)(1 + b) - \exp(-\sigma_s l)(1 - g)(1 - b), \tag{1d}$$

where

$$b = \frac{k_b a_b}{k_s a_s}, g = \frac{k_g a_g}{k_s a_s}, r = (1 - i) \frac{\beta}{2a_s}.$$

$U, V, E$  are complex valued constants,  $\sigma_s = (1 + i) a_s, a_s = (\omega/2\alpha_s)^{1/2}, \alpha_s$  is thermal diffusivity of the sample.

It is the basis to calculate the signal in photothermal detection. The temperature for  $x = 0$  is needed to obtain the signal in microphone one. This distribution can also be used in piezoelectric method after integrating  $T_s(x)$  with the proper limits.

In microphone detection, the incremental pressure produced in photoacoustic chamber is proportional to the temperature [4]:

$$\delta P(t) = \frac{\gamma P_0 T_s(0)}{\sqrt{2} l_g a_g T_0} \tag{2}$$

### 1.2 Temperature Distribution in Blonskij et al’s Model

Independently from Rosenzwaig, Blonskij et al. [6] proposed a solution for temperature distribution in solids for application in piezoelectric detection. In their model, the

periodical modulated light beam impinges on the sample surface  $x = l/2$  and the piezoelectric detector is situated on nonilluminated side of the sample  $x = -l/2$ .

The temperature distribution in the sample can be found from the heat conduction equation:

$$\Delta T - \sigma_s^2 T = -\frac{I\beta}{k} e^{-g^2/b^2} e^{-\beta(l/2-x)} \tag{3}$$

where  $\beta$  is the optical absorption coefficient,  $b$  is the beam radius,  $r^2 = y^2 + z^2$ . The authors took into consideration the average temperature in the  $YZ$  plane and obtained a temperature distribution:

$$T = \frac{I\pi b^2\beta}{k\sigma_s(\beta^2 - \sigma_s^2)} \frac{\beta \cosh(\sigma_s(l/2 + x)) - \beta e^{-\beta l} \cosh(\sigma_s(l/2 - x)) - \sigma_s e^{-\beta(l/2-x)} \sinh \sigma_s l}{\sinh \sigma_s l} \tag{4}$$

Unlike the case of microphone detection, in this case one must use the thermoelastic theory [23,24] to solve the problem. The expression for the electric voltage at the piezoelectric transducer is:

$$V = \frac{e_p L}{\epsilon S} 2\alpha_t \left( \langle T_0 \rangle - \frac{l}{2} \langle \tau \rangle \right) \tag{5}$$

$$\langle T_0 \rangle = \frac{1}{l} \int_{-l/2}^{l/2} T(x) dx \tag{5a}$$

$$\langle \tau \rangle = \frac{12}{l^3} \int_{-l/2}^{l/2} T(x) x dx \tag{5b}$$

where  $L$  is the thickness of the transducer,  $S$  is its surface,  $\alpha_t$  is linear thermal expansion coefficient  $e_p$  is piezomodulus.

In piezoelectric detection one can also apply the temperature distribution previously presented for microphone detection (photoacoustic spectroscopy), but in this case it is necessary to know the full spatial thermal distribution along the sample length in contrary to the temperature of the surface as it is in microphone detection.

Both temperature distributions, R-G's and Blonskij et al's, give the same results using the same parameters to simulations of amplitude and phase spectra.

## 2 Absorption in Semiconductors

Absorption coefficient in ideal, direct band gap semiconductors can be described using two expressions [25]: 1. Urbach tail thermal broadening (associated with parameter  $\gamma$ ) of the absorption band observed in low absorption region:

$$\beta = \beta_0 \exp\left(\frac{(E - E_g) \gamma}{kT}\right), \quad \text{for } E \leq E_g \quad (6)$$

2. absorption connected with the band-to-band, electron transitions:

$$\beta = A_0 (E - E_g)^{1/2}. \quad \text{for } E > E_g \quad (7)$$

Putting expressions (6) and (7) into (1–2) for microphone detection and (4–5) for piezoelectric one, the simulations of amplitude and phase can be obtained for both of these methods.

### 3 Amplitude and Phase of Piezoelectric Spectra

#### 3.1 Ideal Crystal

Figure 1 presents the theoretical predictions for the amplitude (a) and phase (b) of piezoelectric spectra in the rear mode configuration [15], amplitude (c) and phase (d) of piezoelectric spectra in the front mode [15] and amplitude (e) and phase (f) of microphone spectra of the sample of the thickness 1 mm, thermal diffusivity  $0.05 \text{ cm}^2 \cdot \text{s}^{-1}$ ,  $E_g = 2.74 \text{ eV}$ ,  $\gamma = 0.6$  and frequency of modulation 76 Hz. The chosen frequency affects the character of amplitude and phase spectra as it is associated with the thermal diffusion length and depth of signal generation area. It was chosen as a value which gives strong and stable signal in spectroscopic measurements. The

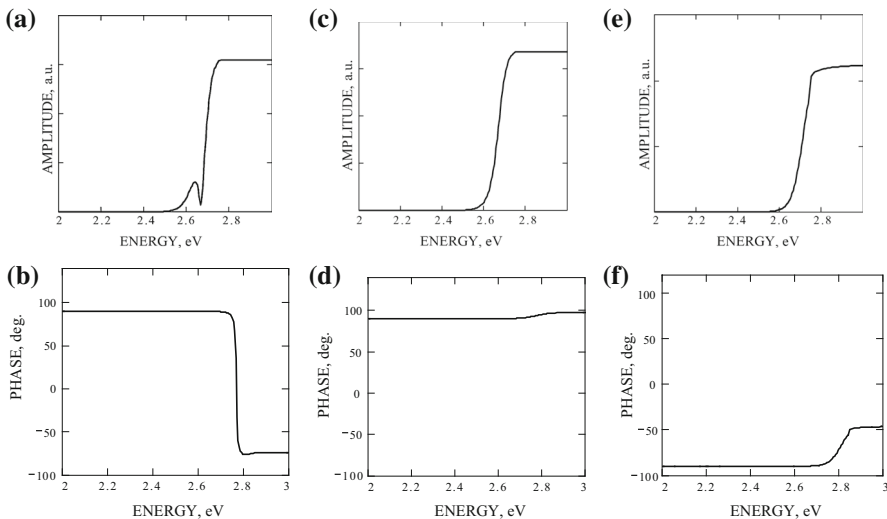


**Fig. 1** Theoretical simulations of the amplitude (a) and phase (b) of piezoelectric spectra in the rear mode configuration, amplitude (c) and phase (d) of piezoelectric spectra in the front mode and amplitude (e) and phase (f) of microphone spectra of sample of the thickness 1 mm, thermal diffusivity  $0.05 \text{ cm}^2 \cdot \text{s}^{-1}$ ,  $E_g = 2.74 \text{ eV}$ ,  $\gamma = 0.6$ . Frequency of modulation 76 Hz

rear and front configurations are associated with the geometry of sample and detector position [6]. The sample is located on the detector. At rear mode, in piezoelectric detection, the sample is irradiated from one side and the detector is located on the other (nonilluminated), at front mode detector is located at the illuminated surface (in Jackson–Amer [6] model it requires the o-ring shaped detector). In Fig. 1, a characteristic peak in the sub-bandgap region in the amplitude spectrum of rear configuration is clearly visible. According to the model, the peak is due to subtracting the components coming from the piston (average expansion of the sample) and drum effects (bending of the sample) [6, 15] in the rear configuration mode. In the phase spectra, this phenomenon is manifested as a sharp change of the phase and crossing the zero value, when the compensation for bending and expansion of the sample occurs. The amplitude spectra for microphone and piezoelectric front mode have very similar waveforms, though the changes in phase for the piezoelectric front mode have a smaller range and the opposite sign to microphone detection case.

### 3.2 Corrections of the Models in the Case of the Presence of Defects

In the case of the presence of defects in the surface and volume, one must take into account the modification of the temperature distribution and additional sources of temperature generation. In this work, only the influence of surface defects that are often observed in semiconductors is considered. The simulation of volume defects contribution to the spectra can be found in reference [18]. It is assumed that the defect level (or levels) of the energy  $E_d$  is present within very thin layer of  $d$  thickness and thermal parameters ( $\sigma_c$ ,  $k_c$ ) different from the volume of the sample is assumed. The absorption coefficient due to the presence of the defect has the Gaussian character:

$$\beta = A_d \cdot \exp\left(\frac{E - E_d}{\beta_1}\right)^2 \quad (8)$$

where  $E_d$  is the value of the energy of the defect and  $\beta_1$  is the parameter describing the width of Gaussian shape maximum,  $A_d$  – amplitude of the maximum.

The nature of the defect levels can be associated with the quality of the surface after the preparation processes (grounding, polishing, etching).

Malinski [9] proposed an approximate model of thermal distribution in this case. An analogous expression to Malinski's can also be obtained for a modified version of Blonskij *et al*'s model taking the assumptions given above. For the energy  $E_d$  of radiation, the layer strongly absorbs, while the volume of the sample is transparent. The temperatures in this layer have the form (for the absorption at opposite surfaces):

$$T_1^d(x) = \frac{I_0(1 - \exp(-\beta d)) [\cosh(\sigma_c(x + \frac{l}{2}))]}{k_c \sigma_c \sinh(\sigma_s l)}, \quad (9)$$

$$T_2^d(x) = \frac{I_0(1 - \exp(-\beta d)) [\cosh(\sigma_c(\frac{l}{2} - x))]}{k_c \sigma_c \sinh(\sigma_c l)}, \quad (10)$$

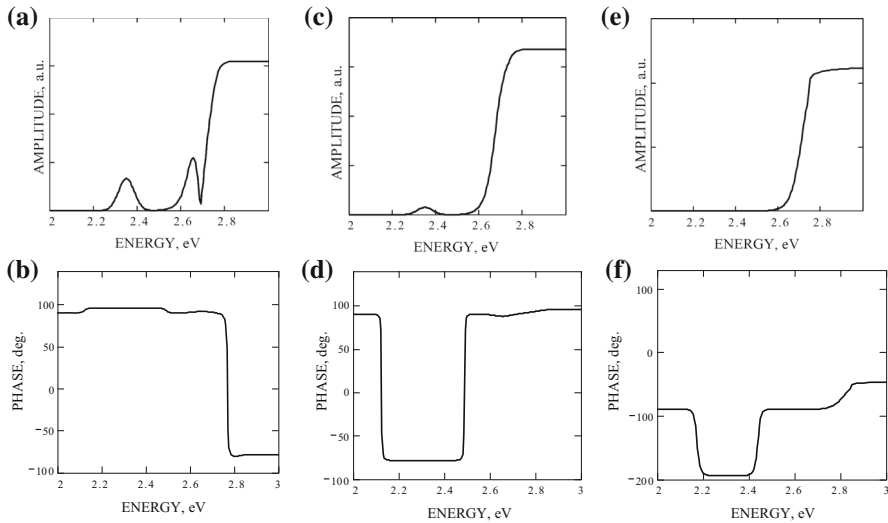


**Fig. 2** Theoretical simulations of the amplitude (a) and phase (b) of piezoelectric spectra in the rear mode configuration, amplitude (c) and phase (d) of piezoelectric spectra in the front mode and amplitude (e) and phase (f) of microphone spectra of the sample with two defects located on the same surface and parameters: energies  $E_1 = 2.35$  eV and  $E_2 = 2.7$  eV, amplitudes  $A_1 = 10$ ,  $A_2 = 22$ , half-width  $\beta_1 = 0.05$  eV,  $\beta_2 = 0.05$  eV, located at the same surface, conductivity of sample  $k_s = 0.19$  W·cm<sup>-1</sup>·K<sup>-1</sup> and defected layer  $k_c = 0.02$  W·cm<sup>-1</sup>·K<sup>-1</sup>. Frequency of modulation 76 Hz

and the temperature distribution in the sample is the sum of temperatures generated in surface and volume of the sample:

$$T'(x) = T(x) + T_1^d(x) + T_2^d \quad (11)$$

where  $T(x)$  is describe by the expression (7).

Putting the corrected expression for temperature distribution (11) into (4, 5) for piezoelectric and (1, 2) for microphone methods, one can obtain the theoretical spectra.

Figure 2 shows amplitude (a) and phase (b) of piezoelectric spectra in the rear mode configuration, amplitude (c) and phase (d) of piezoelectric spectra in the front mode and amplitude (e) and phase (f) of microphone spectra for the same for same parameters as for the ideal crystal ( $E_g, \beta, \gamma$ ) with two defects located on the same surface and parameters: energies  $E_1 = 2.35$  eV and  $E_2 = 2.7$  eV, amplitudes  $A_1 = 10$ ,  $A_2 = 22$ , half-width  $\beta_1 = 0.05$  eV,  $\beta_2 = 0.05$  eV, conductivity of sample  $k_s = 0.19$  W·cm<sup>-1</sup>·K<sup>-1</sup> and defected layer  $k_c = 0.02$  W·cm<sup>-1</sup>·K<sup>-1</sup> and modulation frequency 76 Hz. It is clearly visible that in every spectrum, both amplitude and phase change the character the different way. In amplitude, the biggest influence of defect states is observed for piezoelectric rear detection. In contrast, in microphone amplitude (for the chosen parameters) there is no noticeable change in amplitude. This detection seems to be the least sensitive in amplitude. The influence of the defects is observed for every spectra of the phase, although they introduce the different character of changes for each spectrum.

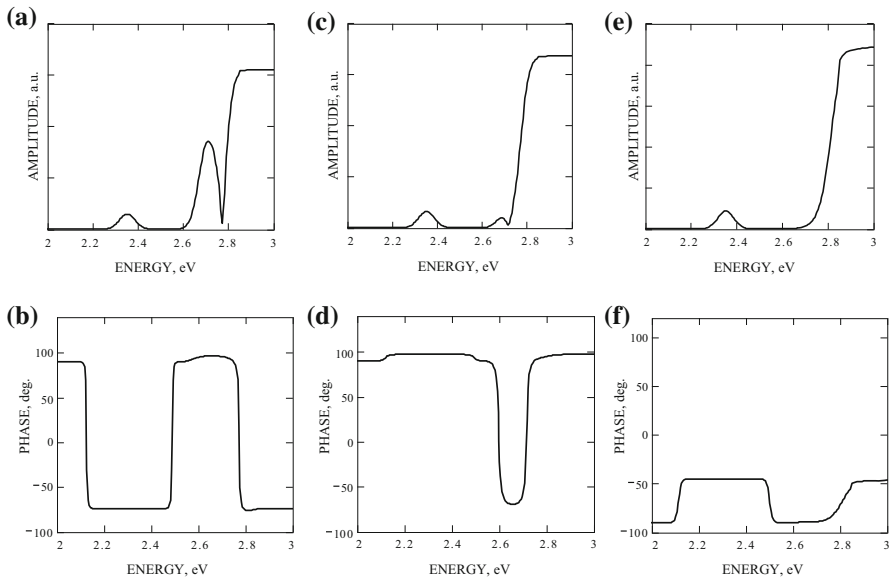


**Fig. 3** Theoretical simulations of the amplitude (a) and phase (b) of piezoelectric spectra in the rear mode configuration, amplitude (c) and phase (d) of piezoelectric spectra in the front mode and amplitude (e) and phase (f) of microphone spectra for the same for same parameters as for Fig. 2, but with one defect ( $E_1$ ) located at the illuminated surface and the second one ( $E_2$ ) located at the nonilluminated surface. Frequency of modulation 76 Hz

Figure 3 shows amplitude (a) and phase (b) of piezoelectric spectra in the rear mode configuration, amplitude (c) and phase (d) of piezoelectric spectra in the front mode and amplitude (e) and phase (f) of microphone spectra for the same for same parameters as for Fig. 2, but with one defect ( $E_1$ ) located at the illuminated surface and the second one ( $E_2$ ) located at the nonilluminated surface.

As in the previous case, the most visible influence of the presence of defects is visible in amplitude of rear mode in piezoelectric detection. The changes are also observed in amplitude of front mode. As before, the smallest changes in amplitude are observed for microphone—only one additional maximum is observed.

In all kinds of detections the phase spectra are more sensitive to the presence of the defect levels.

Comparison of the characteristics of the spectra gives information not only about the position of the defect but also about its thermal parameters and the thickness of the damaged layer. In [18] there was presented the comparison of the above model (for piezoelectric detection) and the one of Fernelius for two-layer system, based on R–G theory, which does not contains above approximations. It was shown that these models in the case of the presence of surface defect give the same qualitative results.

It was assumed that the subsurface damaged layer has different thermal parameters to the rest of the sample. The change of thermal conductivity was assumed to be ten times less than the value of bulk part. The influence of the quality of the subsurface layer on the value of thermal conductivity is a subject of interests [26–28]. The rela-



tion between subsurface defected layer and roughness of the surface in optic active materials was investigated by Li [29]. Cabrero et. al. [30] investigated the influence of irradiation of heavy ions of SiC. Due to this procedure the layer of 10  $\mu\text{m}$  was damaged. The influence of annealing in different temperatures on thermal conductivity was investigated. In the most damaged part of the sample, the value of thermal conductivity was almost one hundred times less than for pure SiC. Depending on the damage of the layer, the increase and decrease in thermal conductivity was observed. The value assumed in simulations seems to be reliable and its real quantity will be estimated in comparison to the experimental data.

## 4 Conclusions

The basic theoretical properties of microphone and piezoelectric photothermal spectroscopy were presented here. Thermal distributions based on Rosencwaig–Gersho and Blonskij et al’s models were analyzed for the interpretation of amplitude and phase spectra of microphone and piezoelectric detection in the case of semiconductors. A waveform of absorption coefficient typical of semiconductors was assumed. Additional assumptions were introduced to simulate surface defects. Both microphone and piezoelectric detections were performed in order to simulate the amplitudes and phases of semiconductor spectra. Comparing these can be useful for determining the nature of defects. Each of the methods: microphone and piezoelectric (for piezoelectric detections, both front and rear modes) gives different waveforms, in terms of amplitude and phase spectra, for fixed parameters and localizations of defects. The amplitude of microphone detection seems to be the least sensitive parameter for detecting the presence of surface defects. Comparison and multiparameter fitting to the experiment results enables determination of optical (energy gap) and thermal (thermal diffusivity, thermal conductivity) parameters of the materials investigated. The thickness of the destroyed layer can also be estimated.

**Open Access** This article is distributed under the terms of the Creative Commons Attribution 4.0 International License (<http://creativecommons.org/licenses/by/4.0/>), which permits unrestricted use, distribution, and reproduction in any medium, provided you give appropriate credit to the original author(s) and the source, provide a link to the Creative Commons license, and indicate if changes were made.

## References

1. Y. Song, D.M. Todorovic, B. Cretin, P. Vairac, *Int. J. Solids Struct.* **47**, 1871 (2010)
2. T. Toyoda, T. Hayakawa, Q. Shen, *Mater. Sci. Eng. B* **78**, 84 (2000)
3. F. Firszt, K. Strzałkowski, J. Zakrzewski, S. Łęgowski, H. Męczyńska, M. Maliński, D. Dumcenco, ChT Huang, Y.S. Huang, *Phys. Status Solidi B* **247**, 1402 (2010)
4. A. Rosencwaig, A. Gersho, *J. Appl. Phys.* **47**, 64 (1976)
5. N. Fernelius, *J. Appl. Phys.* **51**, 650 (1980)
6. W. Jackson, N.M. Amer, *J. Appl. Phys.* **51**, 3343 (1980)
7. I.V. Blonskij, V.A. Tkhoryk, M.L. Shendeleva, *J. Appl. Phys.* **79**, 3512 (1996)
8. C.A. Bennet Jr., R.R. Patty, *Appl. Opt.* **21**, 49 (1982)
9. M. Maliński, *Arch. Acoust.* **27**, 217 (2002)
10. R.S. Quimby, W.M. Yen, *J. Appl. Phys.* **51**, 4985 (1980)

11. L.C.M. Miranda, Appl. Opt. **21**, 2923 (1982)
12. I.N. Bandeira, H. Closs, C.C. Ghizoni, J. Photoacoust. **1**, 275 (1982)
13. V.A. Sablikov, V.B. Sandomirskii, Phys. Status Solidi (b) **120**, 471 (1983)
14. E.K.M. Siu, A. Mandelis, Phys. Rev. B **34**, 7222 (1986)
15. M.D. Dramicanin, Z.D. Ristovski, P.M. Nikolic, D.G. Vasiljevic, D.M. Todorovic, Phys. Rev. B **51**, 14226 (1995)
16. M. Pawlak, M. Malinski, F. Firszt, J. Pelzl, A. Ludwig, A. Marasek, Meas. Sci. Technol. **25**, 035204 (2014)
17. M. Malinski, Ł. Chrobak, Opto-Electron. Rev. **19**, 46–50 (2011)
18. J. Zakrzewski, M. Maliński, K. Strzałkowski, Int. J. Thermophys. **33**, 1228 (2012)
19. T. Nakamura, K. Katayama, H. Mori, S. Fujiwara, Phys. Status Solidi B **241**, 2659 (2004)
20. M. Adachi, K. Ando, T. Abe, N. Inoue, A. Urata, S. Tsutsumi, Y. Hashimoto, H. Kasada, K. Katayama, T. Nakamura, Phys. Status Solidi B **243**, 943 (2006)
21. K. Strzałkowski, Mater. Chem. Phys. **163**, 453 (2015)
22. J. Zakrzewski, M. Malinski, K. Strzałkowski, Int. J. Thermophys. **34**, 725 (2013)
23. S.P. Timoshenko, J.N. Goodier, *Theory of Elasticity* (McGraw-Hill, New York, 1970)
24. A.M. Katz, *Theory of Elasticity* (GITTL, Moscow, 1956)
25. J.I. Pankove, *Optical Processes in Semiconductors* (Dover Publications, Mineola, 1976)
26. D. Terris, K. Joulain, D. Lemonnier, D. Lacroix, P. Chantrenne, Int. J. Therm. Sci. **48**, 1467 (2009)
27. A.S. Verma, B.K. Sarker, S. Sharma, R. Bhandari, V.K. Jindal, Mater. Chem. Phys. **127**, 74 (2011)
28. S.K. Estreicher, T.M. Gibbons, Phys. B **404**, 4509 (2009)
29. S. Li, Z. Wang, Y. Wu, J. Mater. Process. Tech. **205**, 34 (2008)
30. J. Cabrero, F. Audubert, R. Paillet, A. Kusiak, J.L. Battaglia, P. Weisbecker, J. Nucl. Mater. **396**, 202 (2010)